

Evolution of Non-linear Fluctuations in Preheating after Inflation

Yasusada Nambu* and Yohei Araki†

Department of Physics, Graduate School of Science, Nagoya University, Chikusa, Nagoya 464-8602, Japan

(Dated: November 25, 2005)

We investigate the evolution of the non-linear long wavelength fluctuations during preheating after inflation. By using the separate universe approach, the temporal evolution of the power spectrum of the scalar fields and the curvature variable is obtained numerically. We found that the amplitude of the large scale fluctuations is suppressed after non-linear evolution during preheating.

PACS numbers: 04.25.Nx, 98.80.Hw

Keywords: inhomogeneous universe; preheating; back reaction

I. INTRODUCTION

Preheating after inflation is a crucial stage in the early universe. Fluctuations of matter fields and gravitational fields are amplified due to the parametric resonance caused by the coherent oscillation of the inflaton field[1, 2, 3, 4, 5]. One of the important question on preheating is how the long wavelength metric fluctuation is amplified by the parametric resonance. The linear analysis shows that non-adiabatic modes of long wave fluctuations are amplified and grow during preheating until the non-linear effect by the second order fluctuations becomes dominant. When the non-linear effect cannot be neglected, the backreaction of the fluctuations on the evolution of background quantities becomes dominant and the amplification of long wave modes stops [6, 7]. To obtain complete understanding of the evolution of inhomogeneities during preheating, we have to investigate non-linear evolution of fluctuations.

The separate universe approach[8] is an appropriate method to treat the non-linear dynamics of long wavelength fluctuations during preheating. This approach neglects fluctuations of which wavelength is smaller than the Hubble horizon scale. For each spatial point, the basic equation of the separate universe reduces to that of the Friedmann equation for a homogeneous and isotropic flat universe. However, all dynamical variables include non-linear inhomogeneities of which wavelength is larger than the Hubble horizon scale. As the separate universe approach includes all order long wavelength non-linear gravitational fluctuations, we can apply this method to investigate the backreaction effect on evolution of a Friedmann-Robertson-Walker(FRW) universe[9].

Tanaka and Basset[10] investigated preheating using the separate universe approach. They found that initial small fluctuations are amplified and evolve to random spatial distribution. In the separate universe, dynamical variables at each spatial point evolve independently. Hence, in the early stage of evolution, fluctuations keep their initial spatial distribution and only the amplitude of fluctuations grows by the parametric resonance. When the amplitude of the massless field grows to be comparable to that of the inflaton field, the non-linear interaction between scalar fields becomes to be dominant and the system enters a chaotic regime. Then, the field variables at each spatial point behave as independent random variables. At this stage, the power spectrum of fluctuations is same as that of random white noise.

In this paper, we concentrate on the evolution of the power spectrum of fluctuations during preheating especially on curvature fluctuation that gives an impact on formation of large scale structure. By performing the numerical simulation of preheating based on the separate universe approach, we aim to understand the feature of evolution of long wavelength non-linear fluctuation during preheating.

The plan of paper is as follows. In Sec. 2, we review the separate universe approach. In Sec. 3, we analytically estimate the evolution of the power spectrum of scalar fields and a curvature variable. We present our numerical results in Sec. 4 and Sec. 5 is devoted to summary and conclusion. We use units in which $c = \hbar = 8\pi G = 1$ throughout the paper.

II. SHORT REVIEW OF THE SEPARATE UNIVERSE APPROACH

The separate universe approach[8] is the lowest order spatial gradient expansion (GE)[11] that is obtained by neglecting all terms containing the second order spatial derivative terms in the Einstein equation. All dynamical variables keep the spatial dependence that represents large scale inhomogeneities whose wavelength is larger than the Hubble horizon scale. In this

*Electronic address: nambu@gravity.phys.nagoya-u.ac.jp

†Electronic address: araki@gravity.phys.nagoya-u.ac.jp

approach, we assume the following form of the metric :

$$ds^2 = -N^2 dt^2 + e^{2\alpha} d\mathbf{x}^2, \quad (1)$$

where N is a lapse function and α is the logarithm of the scale factor of the universe. For the system with two scalar fields ϕ_i ($i = 1, 2$), the Einstein equation becomes

$$3H^2 = \frac{1}{2} \sum_j \left(\frac{\dot{\phi}_j}{N} \right)^2 + V(\phi_1, \phi_2), \quad (2)$$

$$\partial_i H = -\frac{1}{2N} \sum_j \dot{\phi}_j \partial_i \phi_j, \quad (3)$$

$$\frac{\dot{\alpha}}{N} = H, \quad \frac{\dot{H}}{N} = -\frac{1}{2} \sum_j \left(\frac{\dot{\phi}_j}{N} \right)^2, \quad (4)$$

$$\frac{1}{N} \left(\frac{\dot{\phi}_j}{N} \right)' + 3H \left(\frac{\dot{\phi}_j}{N} \right) + \frac{\partial V}{\partial \phi_j} = 0, \quad (5)$$

where Eq. (2) is the Hamiltonian constraint, Eq. (3) is the momentum constraint, Eq. (4) and Eq. (5) are evolution equations for the scalar factor and scalar fields.

To understand how the spatial inhomogeneity is included in dynamical variables, it is convenient to use the Hamilton-Jacobi method[11]. By introducing the Hubble function $H = H(\phi_1, \phi_2)$ that is a function of scalar fields, the above set of equations can be written

$$3H^2 = 2 \sum_j \left(\frac{\partial H}{\partial \phi_j} \right)^2 + V(\phi_1, \phi_2), \quad (6)$$

$$\partial_i H = \sum_j \frac{\partial H}{\partial \phi_j} \partial_i \phi_j, \quad (7)$$

$$\frac{\dot{\alpha}}{N} = H, \quad (8)$$

$$\frac{\dot{\phi}_j}{N} = -2 \frac{\partial H}{\partial \phi_j}. \quad (9)$$

The solution of the Hamilton-Jacobi equation (6) contains two constants of integration $d_1(\mathbf{x}), d_2(\mathbf{x})$. If these constants do not have spatial dependence¹, the Hubble function $H = H(\phi_1(\mathbf{x}), \phi_2(\mathbf{x}); d_1, d_2)$ satisfies the momentum constraint (7). By differentiating H with respect to d_j , we have other integration of constants $c(\mathbf{x}), f(\mathbf{x})$:

$$e^{3\alpha} \frac{\partial H}{\partial d_1} \equiv e^{-3c(\mathbf{x})}, \quad (10)$$

$$e^{3\alpha} \frac{\partial H}{\partial d_2} \equiv e^{-3c(\mathbf{x})} f(\mathbf{x}). \quad (11)$$

By solving these equations with respect to ϕ_j , we can obtain the scale factor dependence of the scalar fields:

$$\begin{aligned} \phi_1 &= \phi_1(\alpha + c(\mathbf{x}); f(\mathbf{x}), d_1, d_2), \\ \phi_2 &= \phi_2(\alpha + c(\mathbf{x}); f(\mathbf{x}), d_1, d_2). \end{aligned} \quad (12)$$

The gauge invariant variable that reduces to the spatial derivative of the scalar field on the zero curvature gauge is defined by[12]

$$Q_i^{(j)} = \partial_i \phi_j - \phi_{j,\alpha} \partial_i \alpha, \quad (13)$$

¹ The constants d_j can have spatial dependence if they satisfy $H_{,\phi_1} \partial_i d_1 + H_{,\phi_2} \partial_i d_2 = 0$. However, the inhomogeneity caused by d_i is related to the decaying mode of perturbations and sub-dominant. Hence we ignore this type of inhomogeneity here.

and these variables are non-linear generalization of Mukhanov's gauge invariant variable in the linear perturbation. The scalar field equation (5) in the zero curvature slice $\partial_i \alpha = 0$ is

$$\phi_{j,\alpha\alpha} + \left(3 + \frac{H_{,\alpha}}{H}\right) \phi_{j,\alpha} + \frac{V_{,\phi_j}}{H^2} = 0,$$

and by taking the spatial derivative of this equation, it is possible to show that the variable $\mathbf{Q}_i = (Q_i^{(1)}, Q_i^{(2)})$ satisfies the following evolution equation:

$$\begin{aligned} \mathbf{Q}_{i,\alpha\alpha} + \left(3 + \frac{H_{,\alpha}}{H}\right) \mathbf{Q}_{i,\alpha} + \mathbf{M} \mathbf{Q}_i &= 0, \\ ;(\mathbf{M})_{ij} &= \frac{V_{\phi_i \phi_j}}{H^2} - \frac{e^{-3\alpha}}{H} (e^{3\alpha} H \phi_{i,\alpha} \phi_{j,\alpha})_{,\alpha}, \end{aligned} \quad (14)$$

that has the exactly same form as in the linear perturbation case. However, the coefficients of the equations are spatial dependent and this equation describes non-linear evolution of large scale inhomogeneities. The non-linear generalization of the gauge invariant variable in the linear perturbation that reduces to the spatial derivative of the three curvature on the comoving slice is defined by

$$\mathcal{R}_i = \partial_i \alpha - \frac{NH}{\dot{\rho}_{\text{tot}}} \partial_i \rho_{\text{tot}} = \partial_i \alpha - \frac{\sum_j \phi_{j,\alpha} \partial_i \phi_j}{\sum_j \phi_{j,\alpha}^2} = \partial_i \alpha - \frac{H}{\dot{H}} \partial_i H, \quad (15)$$

and this quantity can be written using Q_i :

$$\mathcal{R}_i = - \frac{\sum_j \phi_{j,\alpha} Q_i^{(j)}}{\sum_j \phi_{j,\alpha}^2}. \quad (16)$$

By substituting the solution (12), the gauge invariant quantity \mathbf{Q} becomes

$$\mathbf{Q}_i = \begin{pmatrix} \phi_{1,\alpha} & \phi_{1,f} \\ \phi_{2,\alpha} & \phi_{2,f} \end{pmatrix} \begin{pmatrix} \partial_i c(\mathbf{x}) \\ \partial_i f(\mathbf{x}) \end{pmatrix} - \begin{pmatrix} \phi_{1,\alpha} \\ \phi_{2,\alpha} \end{pmatrix} \partial_i \alpha, \quad (17)$$

and the gauge invariant variable \mathcal{R}_i becomes

$$\mathcal{R}_i = \partial_i \alpha - \partial_i c + \frac{\sum_j \phi_{j,\alpha} \phi_{j,f}}{\sum_j \phi_{j,\alpha}^2} \partial_i f. \quad (18)$$

If we take the zero curvature slice $\partial_i \alpha = 0$,

$$\mathcal{R}_i = -\partial_i c + \frac{\sum_j \phi_{j,\alpha} \phi_{j,f}}{\sum_j \phi_{j,\alpha}^2} \partial_i f. \quad (19)$$

From this formula, we can observe that the curvature fluctuation caused by $c(\mathbf{x})$ does not evolve. This mode corresponds to the adiabatic mode in linear perturbation. The curvature fluctuation caused by $f(\mathbf{x})$ corresponds to the non-adiabatic mode and the evolution of the curvature fluctuation is caused by the non-adiabatic mode of scalar fields fluctuations.

III. EVOLUTION OF INHOMOGENEITIES IN PREHEATING

In this section, we consider a specific inflationary model with the inflaton field ϕ and the massless scalar field χ . The potential is assumed to be

$$V(\phi, \chi) = \frac{\lambda}{4} \phi^4 + \frac{g^2}{2} \phi^2 \chi^2. \quad (20)$$

For $\phi \lesssim m_{pl}$, the inflaton field oscillate coherently about $\phi = 0$ and the evolution of the χ field gets the effect of the parametric resonance. For $g^2/\lambda = 2$ case, the longest wavelength mode $k = 0$ is included in a strong resonance band and the fluctuation grows exponentially in time with Floquet index $\mu \approx 0.238$. Thus, the super-horizon mode is amplified by the parametric resonance. As we are interested in the non-linear evolution of fluctuations, we consider $g^2/\lambda = 2$ case in which the growth rate for $k = 0$ fluctuation is the largest.

A. Analytic approximation

In preheating model defined by (20), the time averaged equation of state of the inflaton fields is same as that of radiation and the evolution of the scale factor is given by

$$e^\alpha \approx \left(\frac{t}{t_0} + 1 \right)^{1/2}, \quad (21)$$

where we choose $\alpha = 0$ at $t = 0$. By introducing the conformal time $\eta = \int dt e^{-\alpha}$ and the conformal variables $\tilde{\phi} = e^\alpha \phi$, $\tilde{\chi} = e^\alpha \chi$, the evolution equations of scalar fields become

$$\begin{aligned} \tilde{\phi}'' + \lambda \tilde{\phi}^3 + g^2 \tilde{\phi} \tilde{\chi}^2 &\approx 0, \\ \tilde{\chi}'' + g^2 \tilde{\phi}^2 \tilde{\chi} &\approx 0, \end{aligned} \quad (22)$$

where $' = d/d\eta$. The curvature variable (19) becomes

$$\mathcal{R}_i \approx -\frac{1}{4} \left(\frac{\eta_0}{\eta} \right)^2 \left[\tilde{\phi}' \partial_i \tilde{\phi} + \tilde{\chi}' \partial_i \tilde{\chi} + O\left(\frac{1}{\eta}\right) \right] \quad (23)$$

The solution of the separate universe can be written as

$$\tilde{\phi} = \tilde{\phi}(\eta, f(\mathbf{x})), \quad \tilde{\chi} = \tilde{\chi}(\eta, f(\mathbf{x})), \quad (24)$$

where $f(\mathbf{x})$ is a spatially dependent constant of integration. We obtain perturbative solution by assuming that the amplitude of $\tilde{\chi}$ is small:

$$\tilde{\phi} = \tilde{\phi}_0 + \tilde{\phi}_1 + \dots, \quad \tilde{\chi} = \tilde{\chi}_1 + \tilde{\chi}_2 + \dots. \quad (25)$$

Then the equations for each order of the perturbation become

$$\tilde{\phi}_0'' + \lambda \tilde{\phi}_0^3 = 0, \quad (26)$$

$$\tilde{\chi}_1'' + g^2 \tilde{\phi}_0^2 \tilde{\chi}_1 = 0, \quad \tilde{\phi}_1 = 0, \quad (27)$$

$$\tilde{\phi}_2'' + 3\lambda \tilde{\phi}_0^2 \tilde{\phi}_2 = -g^2 \tilde{\phi}_0 \tilde{\chi}_1^2, \quad \tilde{\chi}_2 = 0, \quad (28)$$

$$\tilde{\chi}_3'' + g^2 \tilde{\phi}_0^2 \tilde{\chi}_3 = -2g^2 \tilde{\phi}_0 \tilde{\phi}_2 \tilde{\chi}_1. \quad (29)$$

The solution of the background inflaton field $\tilde{\phi}_0$ is given by

$$\tilde{\phi}_0 = c \operatorname{cn}(\lambda^{1/2} c \eta; 1/2) \quad (30)$$

where cn is the Jacobi elliptic cosine, c is the initial value of $\tilde{\phi}_0$. We approximate the elliptic function as follows[13]:

$$\tilde{\phi}_0 \approx c \cos(\tau), \quad \tilde{\phi}_0^2 \approx c^2 [F_0 + F_1 \cos(2\tau)], \quad (31)$$

$$\tau = \frac{2\pi}{T} \lambda^{1/2} c \eta, \quad T = 7.416, \quad F_0 = 0.457, \quad F_1 = 0.4973.$$

The equation of $\tilde{\chi}_1$ becomes the Mathieu equation and $\tilde{\chi}_1$ grows by the parametric resonance:

$$\tilde{\chi}_1 = f e^{\mu\tau} \cos \tau, \quad \mu \approx 0.12 \frac{g^2}{\lambda} \quad (32)$$

where f is a spatially dependent constant of integration which specifies the initial amplitude of $\tilde{\chi}$. The solution up to the third order becomes

$$\tilde{\phi} = \left[c - c_1 \left(\frac{g^2}{\lambda} \right) \frac{f^2}{c} e^{2\mu\tau} \right] \cos(\tau) + (\sin \text{ part} + \text{higher frequency part}), \quad (33)$$

$$\tilde{\chi} = \left[f e^{\mu\tau} - c_2 \left(\frac{g^2}{\lambda} \right) \frac{f^3}{c^2} e^{3\mu\tau} \right] \cos(\tau) + (\sin \text{ part} + \text{higher frequency part}), \quad (34)$$

$$\tau \approx \lambda^{1/2} c \eta,$$

where c_1, c_2 are $O(1)$ numerical factors. At the time given by

$$\eta_* \sim \frac{1}{\mu \lambda^{1/2} c} \ln \left(\frac{c}{f} \sqrt{\frac{\lambda}{g^2}} \right), \quad (35)$$

the amplitude of the higher order perturbation terms grow to be comparable to that of the lower order quantities. At this time, fluctuations of $\tilde{\chi}$ field changes the evolution of $\tilde{\phi}$ field through back reaction effect and the exponential growth of fluctuation of $\tilde{\chi}$ -field is shut off. After this time, non-linearities become dominant.

As the Eq. (22) is a chaotic system, the behavior of the scalar fields becomes chaotic after this time. The time scale (35) depends on the initial value $f(\mathbf{x})$ of $\tilde{\chi}$ -field that is the spatial dependent function. The deviation of the field of neighbouring two spatial points grows exponentially for $\eta < \eta_*$. After $\eta > \eta_*$, as the system is chaotic, the dependence of the initial condition is completely randomized and the spatial distribution of $\tilde{\chi}$ becomes that of white noise[10].

To evaluate the evolution of the power spectrum of $\tilde{\chi}$, we assume the function $f(\mathbf{x})$ that specifies the initial distribution of χ obeys the random Gaussian statistics:

$$f(\mathbf{x}) = \sum_{\mathbf{k}} f_{\mathbf{k}} e^{i\mathbf{k} \cdot \mathbf{x}}, \quad \langle f_{\mathbf{k}_1} f_{\mathbf{k}_2}^* \rangle = f_0^2 \left(\frac{k}{k_c} \right)^n \delta_{\mathbf{k}_1 \mathbf{k}_2} \quad f_{\mathbf{k}} = f_{-\mathbf{k}}^*, \quad (36)$$

where k_c is a cut off of wave number and f_0 defines the amplitude of the power at $k = k_c$. The actual initial power spectrum for the χ -field expected to be produced during inflation in this model is investigated by Zibin et al.[7] Owing to their result, the initial spectrum of χ -field for large scales is given by $n = -3$ and scale invariant. In this paper, as we are interested in feature of non-linear evolutions of fluctuations, we does not fix the value of power index of χ -field. The power spectrum of $\tilde{\chi}$ field is given by

$$\mathcal{P}_{\tilde{\chi}} = (k/k_c)^3 \langle |\tilde{\chi}_{\mathbf{k}}|^2 \rangle \approx C_1 e^{2\mu\tau} \left(\frac{k}{k_c} \right)^{n+3} + C_2 \frac{g^2}{\lambda c^2} e^{4\mu\tau} \left(\frac{k}{k_c} \right)^{2n+6}, \quad (37)$$

where C_1, C_2 are $O(1)$ numerical factors. At $\eta \sim \eta_*$, the amplitude of the fluctuation with the wave number

$$\left(\frac{k_*}{k_c} \right) \sim \left(\frac{\lambda c^2}{g^2} \right)^{\frac{1}{n+3}} \exp \left(-\frac{2\mu\lambda^{1/2} c \eta_*}{n+3} \right). \quad (38)$$

becomes $O(1)$ and non-linear. Once the fluctuation with the wave number k_* becomes non-linear, as the system is chaotic, the coherence beyond the scale $1/k_*$ is lost and the fluctuation with the wave number $k < k_*$ is randomized and behaves as white noise. Thus, the power spectrum for $k < k_*$ becomes that of white noise $\propto k^3$. The evolution of the shape of the power spectrum depends on the value of the initial power index n .

For $n < -3$, as the power of smaller k mode is larger, the smaller k mode (large scale) goes to be non-linear first. At $\eta \sim \eta_*$, fluctuation with the wave number $k < k_*$ reaches non-linear and the power spectrum becomes $\mathcal{P}_{\tilde{\chi}} \sim k^3$. At this time, fluctuation with the wave number $k > k_*$ stays linear and the spectrum keeps its initial shape $\mathcal{P}_{\tilde{\chi}} \sim k^{n+3}$. Thus, the shape of the power spectrum at $\eta \sim \eta_*$ is given by

$$\mathcal{P}_{\tilde{\chi}}(k) \sim \begin{cases} k^3 & (k < k_*) \\ k^{n+3} & (k > k_*) \end{cases} \quad (39)$$

For $n > -3$, large k modes (small scale) goes to non-linear first. Once the smallest scale of the system becomes non-linear at $\eta \sim \eta_*$, the coherence of larger scale fluctuation is lost and the spectrum for all wave number changes to be that of the white noise:

$$\mathcal{P}_{\tilde{\chi}}(k) \sim k^3 \quad (k < k_*) \quad (40)$$

The power spectrum of the curvature variable \mathcal{R}_i is given by

$$\mathcal{P}_{\mathcal{R}_i}(k) \approx C_3 \frac{e^{4\mu\tau}}{\tau^4} \left(\frac{k}{k_c} \right)^{n+5} + C_4 \frac{g^2}{\lambda \mu^2 c^2} \frac{e^{6\mu\tau}}{\tau^4} \left(\frac{k}{k_c} \right)^{2n+8} \quad (41)$$

where C_3, C_4 are $O(1)$ numerical factors. At $\eta \sim \eta_*$, the power spectrum for $n < -3$ is

$$\mathcal{P}_{\mathcal{R}_i}(k) \sim \begin{cases} k^3 & (k < k_*) \\ k^{n+5} & (k > k_*) \end{cases} \quad (42)$$

For $n > -3$, the spectrum at $\eta \sim \eta_*$ is

$$\mathcal{P}_{\mathcal{R}_i}(k) \sim k^3 \quad (k < k_*) \quad (43)$$

We summarize the result of the analytic estimation of the power spectrum in TABLE I.

$n < -3$				$n > -3$			
	$\eta < \eta_*$	$\eta > \eta_*$			$\eta < \eta_*$	$\eta > \eta_*$	
\mathcal{P}_χ	k^{n+3}	k^3	$(k < k_*)$, k^{n+3}	$(k > k_*)$	\mathcal{P}_χ	k^{n+3}	k^3
$\mathcal{P}_{\mathcal{R}_i}$	k^{n+5}	k^3	$(k < k_*)$, k^{n+5}	$(k > k_*)$	$\mathcal{P}_{\mathcal{R}_i}$	k^{n+5}	k^3

TABLE I: Power spectrums of χ and \mathcal{R}_i for 3-dimensional space. The initial χ is scale invariant for $n = -3$.

To compare the numerical calculation performed in the following sections, we present the estimation of the power spectrum for 1-dimensional case (TABLE II). The initial spectrums are assumed to be

$$\mathcal{P}_\chi \propto k^{n+1}, \quad \mathcal{P}_{\mathcal{R}_i} \propto k^{n+3}. \quad (44)$$

$n < -1$				$n > -1$			
	$\eta < \eta_*$	$\eta > \eta_*$			$\eta < \eta_*$	$\eta > \eta_*$	
\mathcal{P}_χ	k^{n+1}	k	$(k < k_*)$, k^{n+1}	$(k > k_*)$	\mathcal{P}_χ	k^{n+1}	k
$\mathcal{P}_{\mathcal{R}_i}$	k^{n+3}	k	$(k < k_*)$, k^{n+3}	$(k > k_*)$	$\mathcal{P}_{\mathcal{R}_i}$	k^{n+3}	k

TABLE II: Power spectrums of χ and \mathcal{R}_i for 1-dimensional space. The initial χ is scale invariant for $n = -1$.

B. Numerical simulation of preheating

To confirm the analytic estimation of the evolution of the power spectrums, we perform 1-dimensional lattice simulation of the separate universe.

By introducing the momentum variables $P_\phi = \dot{\phi}/N$, $P_\chi = \dot{\chi}/N$, our basic equations of the separate universe are

$$3H^2 = \frac{1}{2}(P_\phi^2 + P_\chi^2) + V(\phi, \chi), \quad (45)$$

$$\partial_i H = -\frac{1}{2}(P_\phi \partial_i \phi + P_\chi \partial_i \chi), \quad (46)$$

$$\frac{\dot{\alpha}}{N} = H, \quad \frac{\dot{H}}{N} = -\frac{1}{2}(P_\phi^2 + P_\chi^2), \quad (47)$$

$$\frac{\dot{\phi}}{N} = P_\phi, \quad \frac{\dot{P}_\phi}{N} = -3HP_\phi - \frac{\partial V}{\partial \phi}, \quad (48)$$

$$\frac{\dot{\chi}}{N} = P_\chi, \quad \frac{\dot{P}_\chi}{N} = -3HP_\chi - \frac{\partial V}{\partial \chi}. \quad (49)$$

As the initial condition, we must prepare variables $(H, P_\phi, P_\chi, \phi, \chi)$ that satisfy the Hamiltonian constraint (45) and the momentum constraint (46). We adopt the following form of the initial condition :

$$H = h_0, \quad P_\chi = 0, \quad \chi = \chi_0(x), \quad \phi = \phi_0, \quad (50)$$

where h_0 and ϕ_0 are spatially homogeneous constants and $\chi_0(x)$ is the spatially dependent function that specifies the initial inhomogeneity of the χ -field. We prepare $\chi_0(x)$ as a random Gaussian field:

$$\chi_0(x) = \sum_{k>0} \hat{A}_k \cos(kx + \hat{\theta}_k) \quad (51)$$

where $\hat{\theta}_k$ is a uniform random number in $[0, 2\pi]$ and \hat{A}_k is a random number whose probability distribution is given by the Rayleigh distribution

$$P(A_k) \propto A_k \exp\left(-\frac{A_k^2}{\chi_0(k/k_c)^n}\right) \quad (52)$$

where n is the power index of the field. We choose $k_c = \pi N_{\text{grid}}/L$ where L is the size of the calculating region and N_{grid} is number of grids. This value is the smallest wave number that corresponds to the size of the system. The value of the momentum of the inflaton field is determined by the Hamiltonian constraint (45):

$$P_\phi = [6h_0^2 - 2V(\phi_0, \chi_0(x))]^{1/2}. \quad (53)$$

Once the initial values that satisfy the Hamiltonian constraint and the momentum constraint, these constraints are preserved during temporal evolution.

We then must specify the time slicing condition to evolve the system. The simplest one is the synchronous slicing $N = 1$. In this slice, the evolution equations become

$$\dot{\alpha} = H, \quad \dot{H} = -\frac{1}{2}(P_\phi^2 + P_\chi^2), \quad (54)$$

$$\dot{\phi} = P_\phi, \quad \dot{P}_\phi = -3HP_\phi - \lambda\phi^3 - g^2\phi\chi^2, \quad (55)$$

$$\dot{\chi} = P_\chi, \quad \dot{P}_\chi = -3HP_\chi - g^2\phi^2\chi. \quad (56)$$

One of the other choice is the comoving slice. In this slice, the Hubble parameter H is treated as a time parameter ($t = H$) and the evolution equations become

$$\frac{1}{N} \frac{\partial \alpha}{\partial H} = H, \quad \frac{1}{N} = -\frac{1}{2}(P_\phi^2 + P_\chi^2), \quad (57)$$

$$\frac{1}{N} \frac{\partial \phi}{\partial H} = P_\phi, \quad \frac{1}{N} \frac{\partial P_\phi}{\partial H} = -3HP_\phi - \lambda\phi^3 - g^2\phi\chi^2, \quad (58)$$

$$\frac{1}{N} \frac{\partial \chi}{\partial H} = P_\chi, \quad \frac{1}{N} \frac{\partial P_\chi}{\partial H} = -3HP_\chi - g^2\phi^2\chi. \quad (59)$$

The second equation of Eq. (57) determines the lapse function N . In our numerical calculation, we adopt the synchronous slicing $N = 1$ for the sake of the technical simplicity. We also assume that the α is homogeneous at initial time and we have only non-adiabatic mode of curvature fluctuation initially.

We solve Eqs (54)-(56) using the 4th order Runge-Kutta method.

IV. NUMERICAL RESULTS

The spatial grid number used is $2^{14} = 16384$ and the power spectrums are obtained by taking ensemble average of 100 different calculations for different initial distribution of χ field with the same spectral index. We used the parameter $\lambda = 0.1, g^2 = 0.2, \phi_0 = 0.5, \chi_0 = 10^{-5}, h_0 = 0.03$.

A. flat space case

We first performed the numerical calculation of the scalar fields system in flat space (22) to investigate the evolution of non-linear fluctuation without gravitational effect. We obtained the evolution of the power spectrum of $\tilde{\chi}$ -field numerically.

The local evolution of the inflaton field and the massless field is shown in Fig. 1. The spatial derivative of the fields is calculated for two different initial values $\tilde{\chi}_0 = 0.5 \times 10^{-5}, 10^{-5}$.

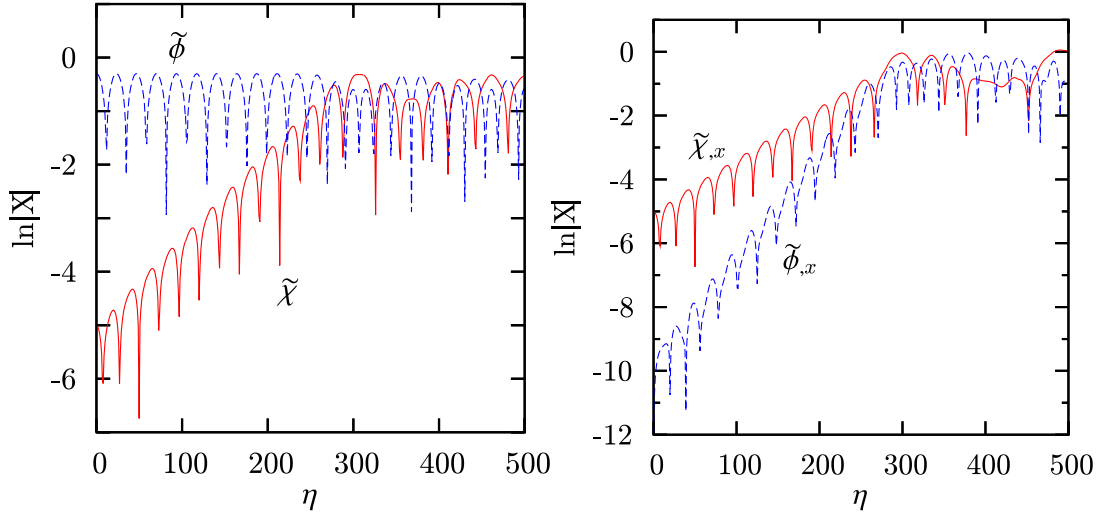


FIG. 1: The left panel shows the evolution of the scalar fields at a specific spatial point. The right panel shows the evolution of the spatial derivative $\tilde{\phi}_{,x}$ and $\tilde{\chi}_{,x}$.

In this calculation, the time scale given by Eq. (35) at which non-linear effect becomes significant, is

$$\eta_* \sim 280.$$

For $\eta \lesssim \eta_*$, the amplitude of $\tilde{\chi}$ field grows exponentially in time by the parametric amplification while the amplitude of $\tilde{\phi}$ field stays constant. In accordance with this behavior, the spatial derivative of $\tilde{\chi}$ and $\tilde{\phi}$ grows exponentially in time. The growth rate of $\tilde{\phi}_{,x}$ is greater than that of $\tilde{\chi}_{,x}$ and at $\eta \sim \eta_*$, $\tilde{\phi}_{,x} \sim \tilde{\chi}_{,x}$. After $\eta \sim \eta_*$, the system enters non-linear regime and the grow of $\tilde{\chi}$, $\tilde{\phi}_{,x}$, $\tilde{\chi}_{,x}$ stops.

We next investigate the evolution of the power spectrum of $\tilde{\chi}$ for different initial power indices.

a. $n = -3$ case Fig. 2 is the evolution of spatial distribution of $\tilde{\chi}$. Initial smooth distribution evolves to random one. Up to η_* , the amplitude of $\tilde{\chi}$ grows keeping its initial distribution. After η_* , $\tilde{\chi}$ begins chaotic behavior and the correlation of the spatial pattern is lost. Fig. 3 shows the evolution of power spectrum of $\tilde{\chi}$. In this case, larger scale has greater power of fluctuation. At $\eta = \eta_* \sim 280$, the fluctuation of the largest scale reaches non-linear and the characteristic scale k_* appears in the form of the power spectrum. For $k < k_*$, the initial power index -3 changes to be 1 that corresponds to white noise. The spectrum for $k > k_*$ keeps its initial slope and a bend at $k = k_*$ appears in the power spectrum. As time goes on, the value of k_* becomes larger and the spectrum for $k < k_c$ becomes that of white noise $\mathcal{P} \propto k$ when k_* reaches k_c . Thus, although the large scale fluctuation reaches $O(1)$ and becomes non-linear temporally, its amplitude decreases to be smaller than unity when the fluctuation with smaller scale reaches non-linear.

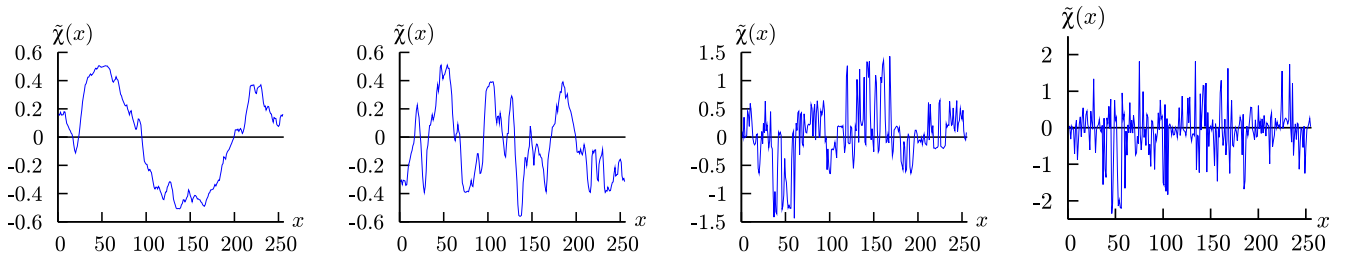


FIG. 2: Evolution of the spatial distribution of $\tilde{\chi}$ field for the initial power index $n+1 = -2$. From the left to the right panel, $\eta = 0, 280, 310, 400$.

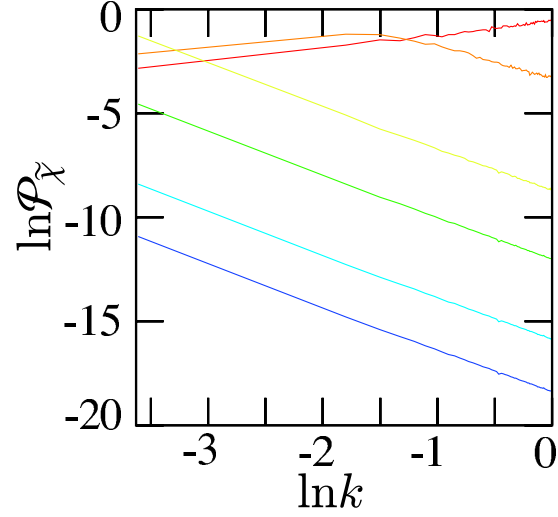


FIG. 3: Evolution of the power spectrum of $\tilde{\chi}$ field for the initial power index $n + 1 = -2$. The spectra at time $\eta = 0$ (blue), 100(cyan), 200(green), 300(yellow), 400(orange), 500(red) are shown.

b. $n = -1$ case In this case, the initial power spectrum of the $\tilde{\chi}$ field is scale invariant. Fig. 4 shows the evolution of spatial distribution of $\tilde{\chi}$ and Fig. 5 shows the evolution of power spectrum of $\tilde{\chi}$. Before η_* , the spectrum evolves keeping its initial power index 0 and all scales goes to non-linear simultaneously at $\eta = \eta_*$. Then the power index changes to be 1 for all k . As the same as $n = -3$ case, the power of the large scale fluctuation is suppressed after the amplitude of the fluctuation reaches non-linear.

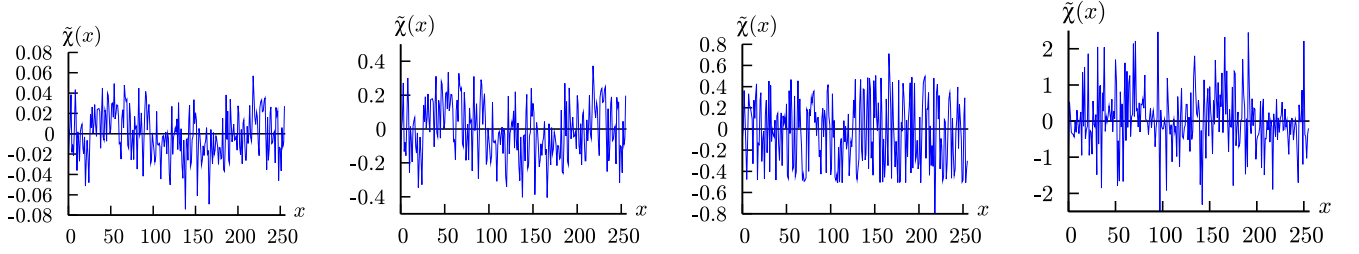


FIG. 4: Evolution of the spatial distribution of $\tilde{\chi}$ field for the initial power index $n + 1 = 0$. From the left to the right panel, $\eta = 0, 260, 300, 400$.

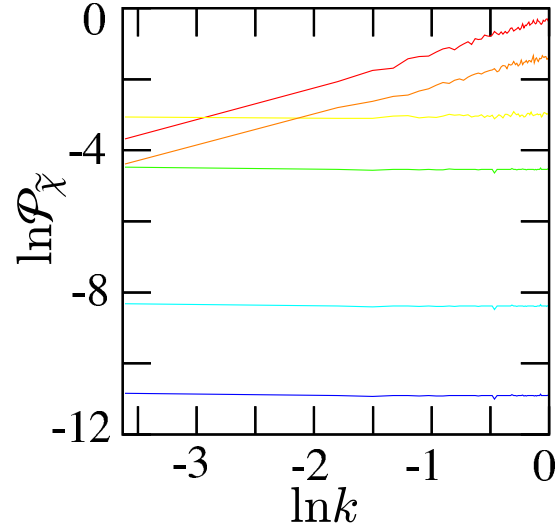


FIG. 5: Evolution of the power spectrum of $\tilde{\chi}$ field for the initial power index $n + 1 = 0$ at $\eta = 0$ (blue), 100(cyan), 200(green), 300(yellow), 400(orange), 500(red).

c. $n = 0$ case In this case, the initial spectrum is same as that of white noise and the small scale reaches non-linear first. Fig. 6 shows the evolution of spatial distribution of $\tilde{\chi}$ and Fig. 7 shows the evolution of power spectrum of $\tilde{\chi}$. As the initial spectrum is same as that of white noise, the power index does not change during whole evolution.

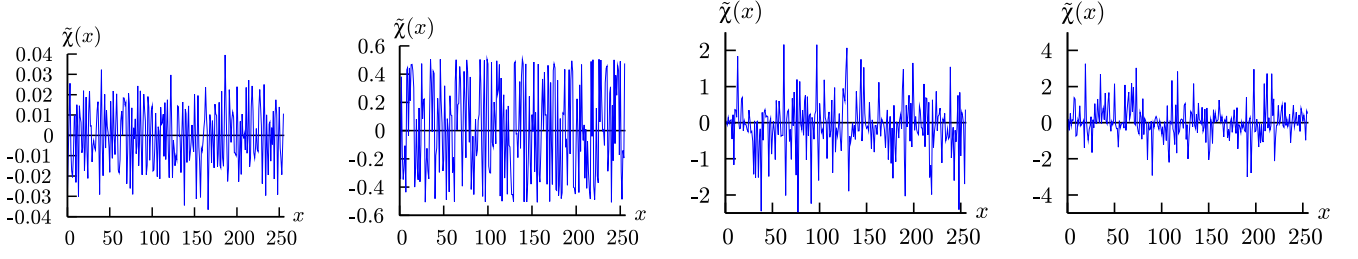


FIG. 6: Evolution of the spatial distribution of $\tilde{\chi}$ field for the initial power index $n + 1 = 1$. From the left to the right panel, $\eta = 0, 100, 200, 300$.

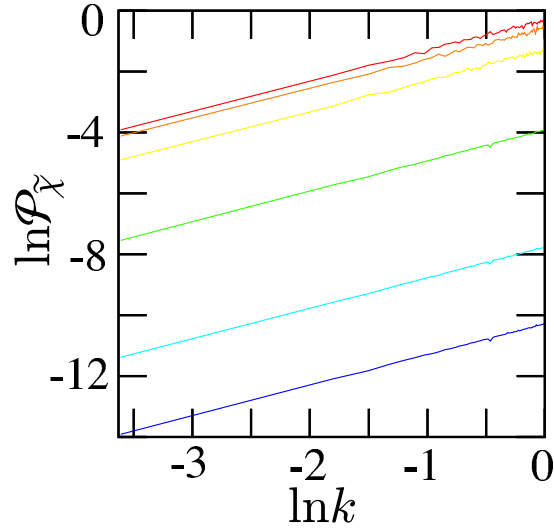


FIG. 7: The power spectrum of $\tilde{\chi}$ field for the initial power index $n + 1 = 1$ at $\eta = 0$ (blue), 100(cyan), 200(green), 300(yellow), 400(orange), 500(red).

d. $n = 1$ case In this case, the initial power index is larger than that of the white noise. Fig. 8 shows the evolution of spatial distribution of $\tilde{\chi}$ and Fig. 9 shows the evolution of power spectrum of $\tilde{\chi}$. After the small scale reaches non-linear, the initial power index 2 reduced to be 1.

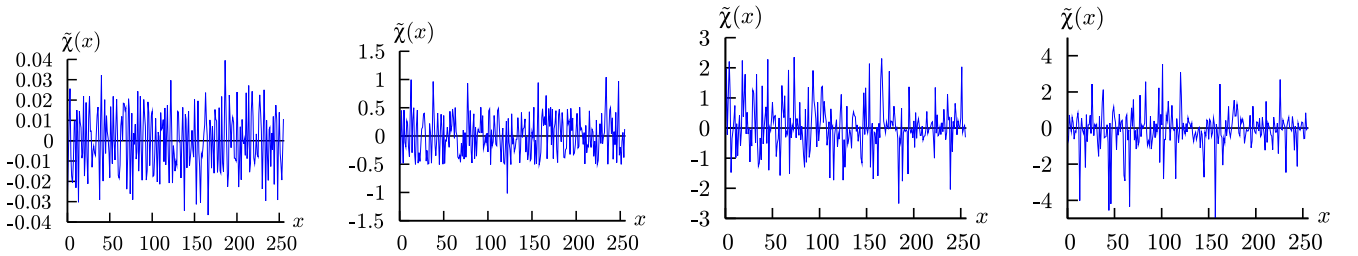


FIG. 8: Evolution of the spatial distribution of $\tilde{\chi}$ field for the initial power index $n + 1 = 2$. From the left to the right panel, $\eta = 0, 260, 300, 400$.

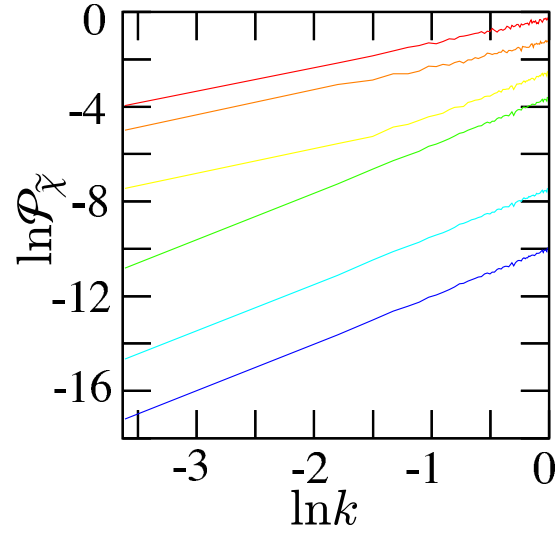


FIG. 9: Evolution of the power spectrum of $\tilde{\chi}$ field for the initial power index $n + 1 = 2$ at $\eta = 0$ (blue), 100(cyan), 200(green), 300(yellow), 400(orange), 500(red).

B. Cosmological case

We next solve Eqs (54), (58), (56), and investigate the evolution of the long wavelength metric fluctuations. The behavior of variables at a specific spatial point is shown in Fig. 10 and Fig. 11.

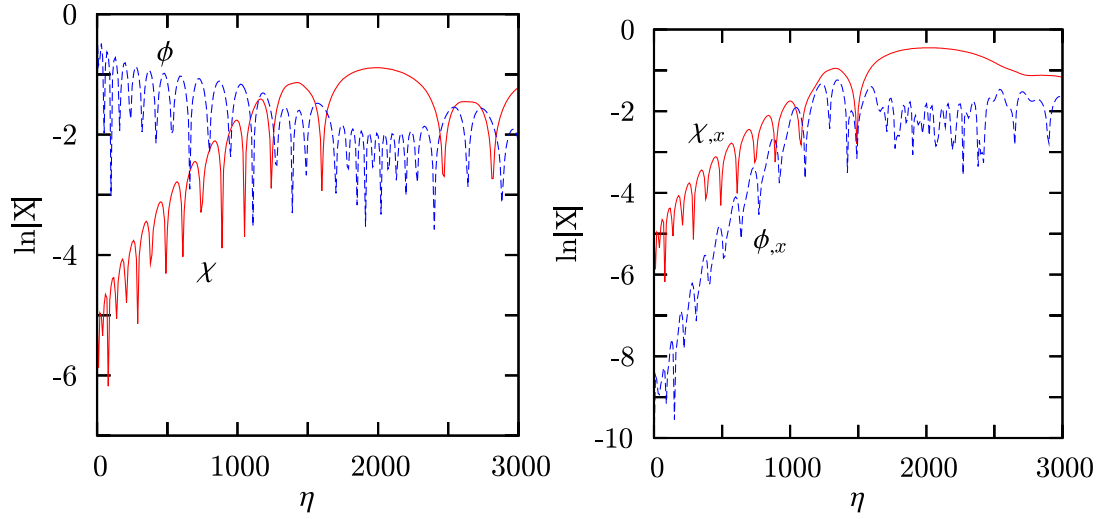


FIG. 10: In the left panel, evolution of scalar fields at a specific spatial point is shown. In the right panel, evolution of the spatial derivative of the scalar fields is shown.

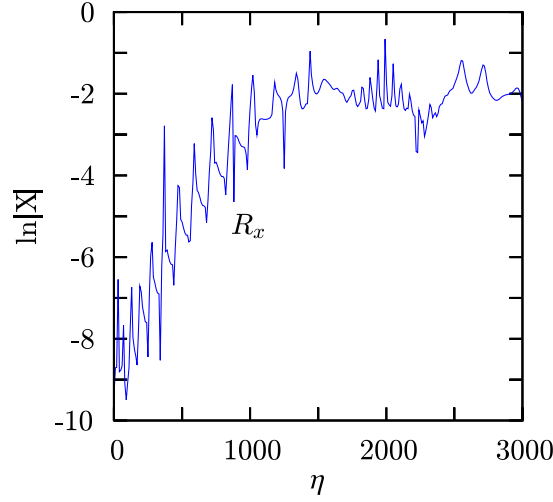


FIG. 11: Evolution of the curvature variable \mathcal{R}_i at a specific spatial point.

The characteristic cosmic time when the system becomes non-linear is given by

$$t_* = -\frac{1}{2H_0} + \frac{H_0}{2}\eta_*^2 \sim 1460.$$

Until this time, $\chi_{,x}$ grows exponentially in conformal time and $\phi_{,x}$ also grows exponentially in accord with the growth of $\chi_{,x}$ with larger growth rate than that of $\chi_{,x}$. We must take care that the amplitude of the spatial derivative of the scalar fields does not reach unity at $t \sim t_*$. This is due to the suppression of the cosmic expansion but the non-linear regime begins at t_* . At $t \sim t_*$, $\chi_{,x} \sim \phi_{,x}$ and the back reaction of χ on the evolution of ϕ begins to be significant and the growth of the fluctuation caused by the parametric resonance stops. The evolution of metric variables H, α, \mathcal{R}_i is same as the evolution of $\chi_{,x}$ and they grow until $t \sim t_*$ when the back reaction cannot be neglected.

Evolution of the power spectrums of χ and \mathcal{R}_i depends on the initial power index of the χ field. The evolution of the power spectrum of χ is qualitatively same as the flat space case. For $n = -3$ (Fig. 12), until $t \sim t_*$, the spectrum of \mathcal{R}_i keeps its initial flat shape k^0 . At $t \sim t_*$, the large scale fluctuation of χ field goes to be non-linear and the bend of the spectrum of \mathcal{R}_i at $k = k_*$ appears. The spectrum of \mathcal{R}_i becomes k for $k < k_*$. The amplitude of the curvature variable \mathcal{R}_i stays less than unity during whole evolution.

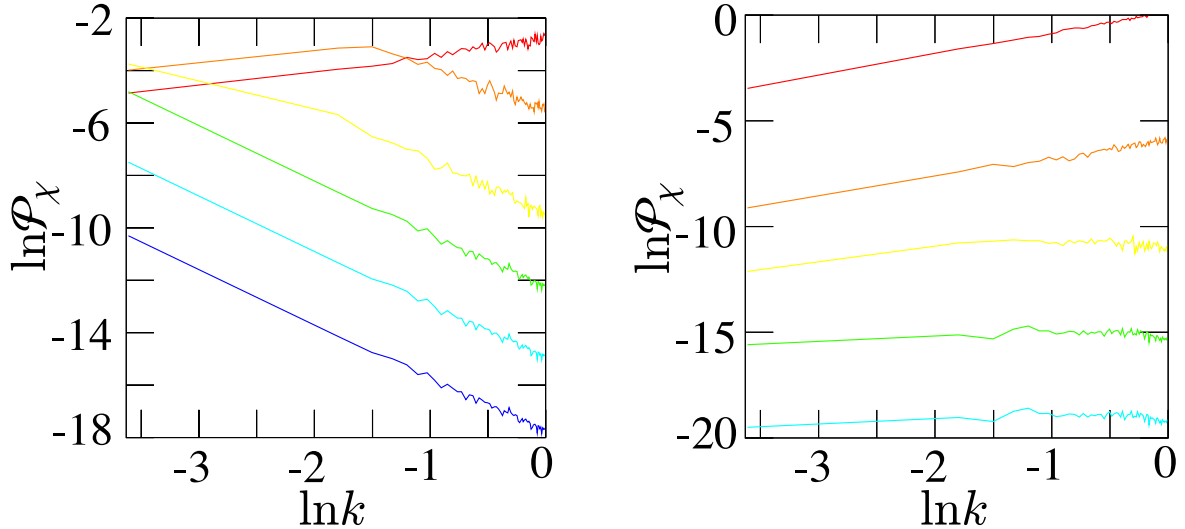


FIG. 12: Evolution of the power spectrums for the initial power index $n + 1 = -2$ case. The left panel is \mathcal{P}_χ and the right panel is $\mathcal{P}_{\mathcal{R}_i}$. Time is $t = 0$ (blue), 400(cyan), 800(green), 1200(yellow), 1600(orange), 2000(red).

For $n \geq -1$ (Fig. 13, Fig. 14, Fig. 15), until $t \sim t_*$, the spectrum of \mathcal{R}_i keeps its initial shape k^{n+3} . At $t \sim t_*$, the small scale

fluctuation of χ field goes to be non-linear and after this time, the spectrum of \mathcal{R}_i becomes k for all wave number. The amplitude of the curvature variable \mathcal{R}_i stays less than unity during whole evolution.

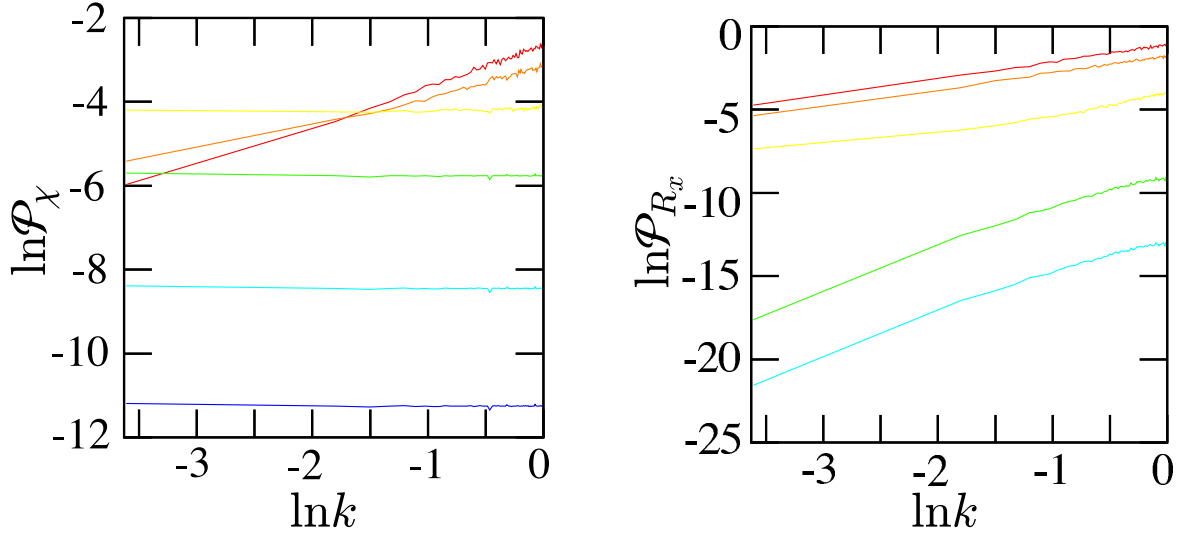


FIG. 13: Evolution of the power spectrums for the initial power index $n + 1 = 0$ case. The left panel is \mathcal{P}_χ and the right panel is $\mathcal{P}_{\mathcal{R}_i}$. Time is $t = 0$ (blue), 400(cyan), 800(green), 1200(yellow), 1600(orange), 2000(red).

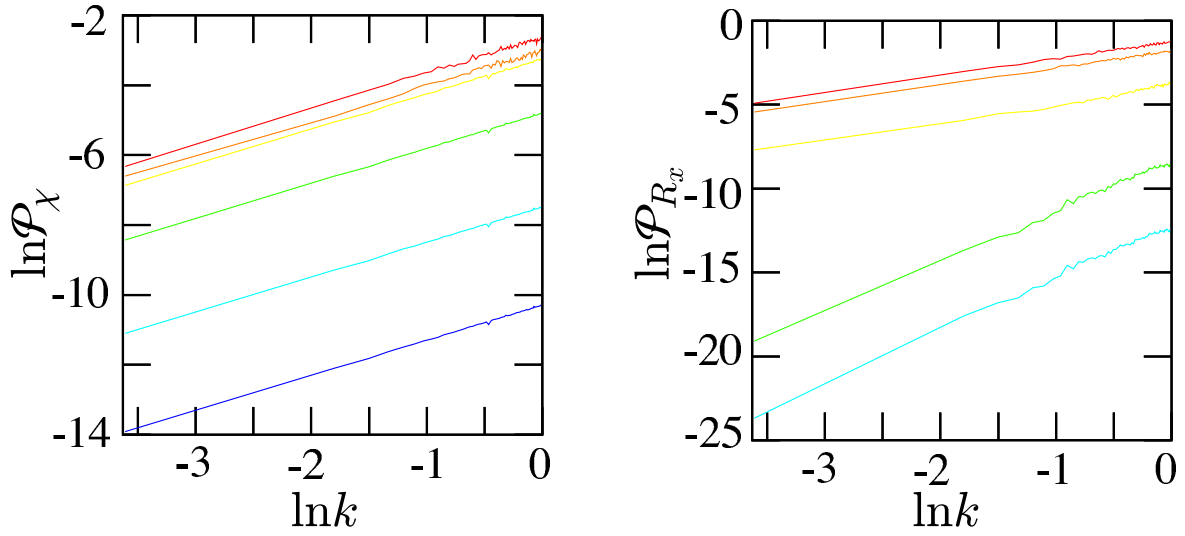


FIG. 14: Evolution of the power spectrums for the initial power index $n + 1 = 1$ case. The left panel is \mathcal{P}_χ and the right panel is $\mathcal{P}_{\mathcal{R}_i}$. Time is $t = 0$ (blue), 400(cyan), 800(green), 1200(yellow), 1600(orange), 2000(red).

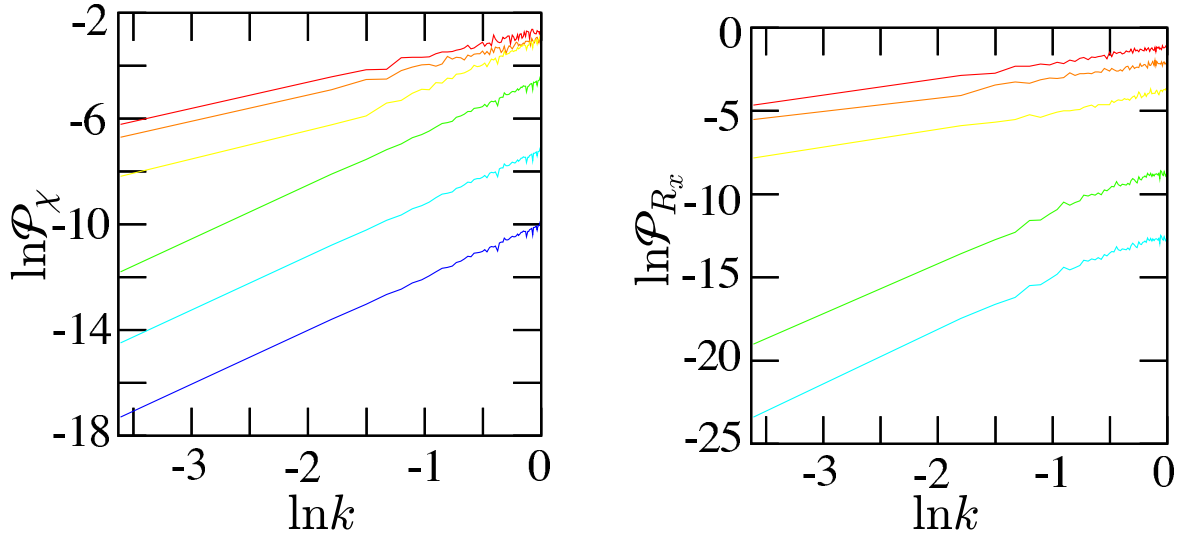


FIG. 15: Evolution of the power spectrums for the initial power index $n + 1 = 2$ case. The left panel is \mathcal{P}_χ and the right panel is \mathcal{P}_{R_i} . Time is $t = 0$ (blue), 400(cyan), 800(green), 1200(yellow), 1600(orange), 2000(red).

V. SUMMARY AND DISCUSSION

In this paper, we investigated the evolution of long wavelength fluctuations during preheating after inflation. By using the separate universe approach, we obtained the evolution of the power spectrum of long wavelength fluctuations numerically. During the linear stage of the evolution, the fluctuation of the massless field grows exponentially in time by the parametric amplification, but the power spectrum keeps its initial shape. When the fluctuation of the massless field becomes non-linear, the amplification of fluctuations stops by the back reaction effect of massless field on the inflaton field. After this time, the system enters the chaotic non-linear stage and the shape of the spectrum changes. For large scale mode, the amplitude of the fluctuation is suppressed because the statistical nature of the large scale mode becomes that of white noise after the non-linear evolution. The evolution of the curvature variable that has an important role in the cosmological scenario is qualitatively same as the evolution of the scalar field fluctuations. Hence we do not expect the significant effect of the parametric amplification during preheating on the evolution of the large scale fluctuations of metric variables. On the other hand, for small scale fluctuations, the power grows for larger k and this leads to the possibility of the formation of the non-linear structures such as primordial black holes[14].

Acknowledgments

This work was supported in part by a Grant-In-Aid for Scientific Research of the Ministry of Education, Science, Sports, and Culture of Japan (11640270).

-
- [1] Traschen J and Brandenberger R H 1990 Particle production during out-of-equilibrium phase transitions Phys. Rev. D 42 2491–2504
 - [2] Kofman L, Linde A and Starobinsky A 1994 Reheating after Inflation Phys. Rev. Lett. 73 3195–3198
 - [3] Kodama H and Hamazaki T 1996 Evolution of Cosmological Perturbations in a Stage Dominated by an Oscillatory Scalar Field Prog. Theor. Phys. 96 949–970
 - [4] Nambu Y and Taruya A 1997 Evolution of Cosmological Perturbation in Reheating Phase of the Universe Prog. Theor. Phys. 97 83–89
 - [5] Taruya A and Nambu Y 1998 Cosmological Perturbation with two scalar fields in Reheating after Inflation Phys. Lett. B428 37–43
 - [6] Basset B and Viniegra F 2000 Massless metric preheating Phys. Rev. D 62 043507
 - [7] Zibin J P, Brandenberger R H and Scott D 2001 Backreaction and the parametric resonance of cosmological fluctuations Phys. Rev. D 63 043511
 - [8] Wands D, Malik K A, Lyth D H and Liddle A R 2000 New approach to the evolution of cosmological perturbations on large scales Phys. Rev. D 62 043527
 - [9] Nambu Y 2005 The separate universe and the backreaction of long wavelength fluctuations Phys. Rev. D 71 084016:1–5
 - [10] Tanaka T and Basset B 2003 Application of the Separate Universe Approach to Preheating astro-ph/0302544
 - [11] Salopek D S and Stewart J M 1992 Hamilton-Jacobi theory for General Relativity with Matter Fields Class. Quantum Grav. 9 1943–1967

- [12] Rigopoulos G I and Shellard E P S 2003 Separate Universe Approach and the Evolution of Nonlinear Superhorizon Cosmological Perturbations *Phys. Rev. D* 68 123518:1–8
- [13] Greene P B, Kofman L, Linde A and Starobinsky A A 1997 Structure of resonance in preheating after inflation *Phys. Rev. D* 56 6175–6192
- [14] Suyama T, Tanaka T, Basset B and Kudoh H 2005 Are black holes overproduced during preheating? *Phys. Rev. D* 71 063507